Journal of Hydroscience and Hydraulic Engineering
Vol. 16, No. 1, May, 1998, 73-86

ANALYSIS OF EXPERIMENTAL BED TOPOGRAPHY DATA WITH RESONANCE CONDITIONS IN MEANDERING CHANNELS USING LINEAR THEORIES

By

K. Hasegawa
Hokkaido University, Civil and Environmental Engineering, N13, W8, Sapporo, Japan

K. Nakamura
Incorporated Company Kajima

and

T. Toyabe
Civil Engineering Research Institute, Hokkaido Development Bureau,

SYNOPSIS

Resonance conditions of a bed in a meandering river channel are discussed through the comparison of the experimental data with the linear theories of Parker and Johannesson (10) and Hasegawa (5). The experimental data used in the analysis are provided by Toyabe et al. (13,14) investigation of bed topography in channels of varying radii and meander length. Conclusions from the analysis are : (1) the amplitude, as predicted by linear theories, of a resonant bed wave of fundamental mode is not significantly different from those under other conditions; (2) a bell-shaped frequency response of wave amplitude is evident from both the experimental data and the results of theories applied to cases of both formation and nonformation of bars; and (3) the linear solution for phase lags between the channel meander patterns and the river bed waves agrees reasonably well with the experimental data.

INTRODUCTION

When alternating bars form coincidentally with the effect of bends in a meandering channel, a so-called resonance phenomenon occurs. Early, Kinoshita (8) pointed out this interactions between alternating bars and channel bends as the inherent nature of river channels, and Engelund (3) discussed the coexistence of alternating bars and point bars. However, neither researcher referred to this as resonance. Blondeaux and Seminara (1) and Struiksma et al. (12) almost simultaneously discovered the phenomenon of resonance. Blondeaux and Seminara (1) showed the existence of a resonant frequency, in which the amplitude goes to infinity in the linear equations for the deformation of the bed topography in meandering river channels. Struiksma et al. (12) reported over-deepening of bed at the entrance to a bend being based on their measurements and numerical analyses. Later, Parker and Johannesson (10) formulated a spatial oscillation equation that is easily understandable for the response of bed forms, and showed that the equation can describe the resonance phenomenon. According to their analyses, deformation of bed topography in meandering channels results in a forced oscillation problem where an external force, produced by the channel bend, acts on the free oscillation of bed related to the formation of alternating bars. Over-deepening is a transient response problem,

in which a step function is incorporated into the forcing terms, at an entrance to the bend. Previously, Hasegawa (5) conducted a very similar linear analysis, but did not point out a resonance phenomenon.

The linear equation predicts that the response amplitude approaches infinity for the resonant wavelength. This is contradictory to the real phenomenon. Seminara and Tubino (11) developed the nonlinear analysis by using perturbation method around a singular point, which is corresponding to the resonant wavelength and the resonant width-depth ratio. They obtained an amplitude response that was close to the actual values. This study was based on a finite amplitude theory of the bar height of Colombini et al. (2) and on a nonlinear theory of the interactions between alternate bars and point bars of Seminara and Tubino (11). However, the equations they formulated involve an excessive number of terms and are very complex. Linear analyses are superior to those nonlinear theories in the plain explanation of the mechanism of sand bar formation in a channel bend.

In the Civil Engineering Research Institute of the Hokkaido Development Bureau, Toyabe et al.(13, 14) conducted 80 experiments, consisting of varying wavelengths, maximum curvature, and width-depth ratios. They also made quasi-three-dimensional numerical analyses which retain all nonlinear terms and summarized the characteristics necessary to confirm the significance of the resonance phenomenon for river training. Their experimental results (hereafter referred to as "the experiment") and numerical analysis showed an increase in depth of the scour in meandering channels with the resonant wavelength. However, the increase scour depth was not significantly larger when compared with other typical scours.

In this paper, the experimental results of Toyabe et al.(13,14) are compared with the more easily comprehensible linear theory to re-examine the mechanism of resonance phenomena, and to clarify the limit of the application of the linear theory.

CHARACTERISTICS OF WAVENUMBERS OF THE EQUILIBRIUM BED TOPOGRAPHY

The experiments were comprised of two different radius of curvature-channel width ratios R/B (R: the radius of curvature, B: the channel width) of 5.0 and 10.0. In each case, the channels with eight different wavelength-channel width ratios $\tilde{\lambda}/B$ ($\tilde{\lambda}$: the meandering wavelength) ranging from 6.28 to 31.4 were used. The channel width was fixed at 30 cm. Centerline planforms of the channels were sine-generated curves. The type of sand used was constant for all experiments and had an average grain diameter of 0.056 cm. The discharge and river bed gradient were adjusted to yield channel width-flow depth ratios B/H (H: the average water depth) of 10 , 20, 30 and 40 . Thus, both R/B ratios were studied under conditions with and without alternate bars. After reaching equilibrium, the water surface and bed topography were measured by an automatically controlled bed profiler.

A double Fourier analysis was applied to the bed topography data. In the analysis, the primary wavelength in the transverse direction was set at twice the length of the channel width, and the primary wavelength in the downstream direction was set at the wave length of the channel meander. Mode numbers in the transverse and the downstream direction are represented by i and j, respectively. Dominance of the amplitude components was often observed at (i, j) = (1, 1), (2, 0), (3, 1), (2, 2) (Hasegawa and Nakamura (6, 7)). These results agreed with the experimental results of Hasegawa (5), but they did not completely agree with the results of Garcia et al. (4), which indicated that (1, 1), (2, 0), (1, 2), (1, 3) were dominant. Comparing all the experimental values of these major amplitudes normalized by the water depth, the (2, 0) and (3, 1) waves had almost consistent features regardless of the conditions of the channel. Their amplitude increased as B/H increased, while the (2, 2) wave was largely affected by the topography of the channel, such as $\tilde{\lambda}/B$ and B/H. The (1, 1) wave, which had the largest amplitude, also varied with $\tilde{\lambda}/B$. The amplitude was large when $\tilde{\lambda}/B$ was between 10 and 20, but it decreased as $\tilde{\lambda}/B$ moved away from this range. This wave is meaningful since it is directly affected by the curvature of the channel. Indeed, this is the only component wave which has a resonance relation against the meandering channel form from a view point of the linear

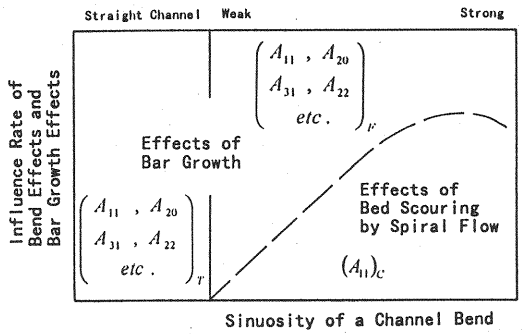

Fig. 1 Conceptual figure for each component of bed wave amplitude
(A)T: amplitude components for an alternating bar in a straight channel
(A)F: amplitude components for an alternating bar affected by a channel bend
(A)C: amplitude components for bed scouring by spiral flow in a channel bend

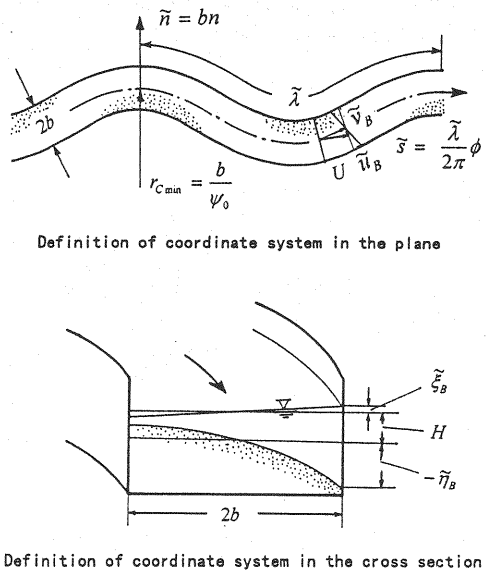

Fig. 2 Definition of coordinate systems in the plane and in the cross section

theory. This is discussed later.

Now, bed topography formed in a meandering channel is thought to be composed of two components: [1] deformed alternating bar influenced by the channel bend, and [2] bed scouring caused by the spiral (secondary) flow in a channel bend. Fig. 1 shows the overall concept for a forming process with respect to each dominant wave amplitude in a meandering channel. The lateral axis indicates the degree of sinuosity of a channel bend, and the vertical axis presents the influence rate of bend effects and bar growth effects on the bed wave forming. The dash line shown in the figure is an imaginary boundary to divide the extension where effects of bend on the bed are dominant i.e. influences of spiral (secondary) flow prevailed over those of an alternating bar formation. Symbols like A_{11}, A_{20} etc. mean the amplitude of (1,1) wave, (2,0) wave etc., respectively. Subscripts T, F and C mean effect of alternating bar formation in a straight channel, effect of alternating bar formation affected by a channel bend and effect of a channel bend itself, respectively. The amplitudes of the (2, 0) and (3, 1) waves in the meandering channel $(A_{20})_F$ and $(A_{31})_F$ are scarcely influenced by the bend. They differ very little from the amplitudes of the straight channel $(A_{20})_T$ and $(A_{31})_T$. But the value of $(A_{22})_F$ is not equal to $(A_{22})_T$ because of indirect effects of the bend. The amplitude of the (1 ,1) wave (A_{11}) is composed of the amplitude of the sand bar $(A_{11})_F$ which is affected by the bend, and $(A_{11})_C$ which is caused by the direct influence of the bend. Only $(A_{11})_F$ is subject to resonance. The effects of channel bends and alternating bars can be independently treated with the linear theory, which allows a linear summation of the two solutions later.

THE LINEAR THEORY AND RESONANCE CONDITIONS

Resonance Conditions of Parker and Johannesson

Parker and Johannesson (10) formulated linear equations of meandering channels. They produced these equations by combining the depth-averaged longitudinal and transverse momentum equations, the continuous equation of flow, the continuous equation of sediment, and the bed load function. They succeeded in comprehensive explanations easily understood by dividing these linear equations into the "F" problem, where alternate bars are treated as affected by the bend, and the "C"

problem, where sand waves are regarded as directly influenced by the bend. The equations in the "F" problem are written as follows:

$$ru_F'+2Pu_F+P_1\eta_F=0 \tag{1}$$

$$ru_F'-r\eta_F'+\frac{\partial v_F}{\partial n}=0 \tag{2}$$

$$rMu_F'+rM_1\eta_F'+\frac{\partial v_F}{\partial n}-\Gamma\frac{\partial^2\eta_F}{\partial n^2}=-r(M-1)u_C'+r(M_1+1)h_C' \tag{3}$$

$$v_F|_{n=\pm1}=0 \quad , \quad \frac{\partial\eta_F}{\partial n}|_{n=\pm1}=0 \tag{4}$$

Where, the used symbols are defined as follows: The prime denotes the differentiation with respect to ϕ; $\phi=2\pi\tilde{s}/\tilde{\lambda}$; $\tilde{s}$ = the longitudinal coordinate along the centerline of channel; $\tilde{\lambda}$ =the meander length; $n=\tilde{n}/b$; $\tilde{n}$= the transverse coordinate; b = the half width of the channel; $r=2\pi H/(\tilde{\lambda}C_{f0})$; H = the depth of the base flow; C_{f0}= the frictional coefficient for the mean flow; $(u_F,v_F,\eta_F)=(\tilde{u}_F/\psi_0U,\tilde{v}_F/\psi_0U,\tilde{\eta}_F/\psi_0H)$; $(\tilde{u}_F,\tilde{v}_F,\tilde{\eta}_F)$= (the perturbations of flow velocity in the longitudinal direction, those in the transverse direction and displacement of the bed topography, all of which are affected by the deformed sand bar due to the bend); $\psi_0=b/\tilde{r}_{C\min}$; $\tilde{r}_{C\min}$= the minimum centerline radius of curvature; U= the cross-sectional mean velocity of the base flow; $u_C=\tilde{u}_C/\psi_0U=n(\tilde{a}_C\cos\phi+\tilde{b}_C\sin\phi)$; $h_C=\tilde{h}_C/\psi_0H=(A+F^2)n\sin\phi$; $(\tilde{u}_C,\tilde{h}_C)$ = (the perturbation of the longitudinal velocity and water depth affected by the channel bend); $(\tilde{a}_C,\tilde{b}_C)$= the parameters of the secondary approximate solution of Engelund (3) related to $\tilde{u}_C$, the excess velocity from the cross-sectional mean velocity, and they are described as follows,

$\tilde{a}_C=-r\frac{2P+\tilde{A}}{r^2+4P^2}$; $\tilde{b}_C=\frac{2P\tilde{A}-r^2}{r^2+4P^2}$; $\tilde{A}=P_1(F^2+A)+A_s-1$; $A=\frac{7.51(\chi+2/7)}{\beta\chi}$; F = the Froude number of the base flow; $P\approx 1$; $P_1=1+5\sqrt{C_{f0}}$; $A_s=181\frac{2\chi^2+4\chi/5+1/15}{(b/H)^2\chi_1}$;

$\chi_1=\frac{1}{13\sqrt{C_{f0}}}$; $\chi=\chi_1-\frac{1}{3}$; $\beta=\frac{1+\alpha_*\mu}{f_*\mu}\sqrt{\frac{\tau^*_c}{\tau^*_{s0}}}$; $M=3/(1-\tau^*_c/\tau^*_{s0})$; $M_1=2.5\sqrt{C_{f0}}M$;

$\Gamma=\frac{\beta}{(b/H)^2C_{f0}}$; $\alpha_*=0.85$; μ= the dynamic Coulomb coefficient; $f_*=1.19$ (when $\mu=0.43$);

τ^*_c =the dimensionless critical shear stress; τ^*_{s0} = the dimensionless shear stress for the base flow.

The system composed of Eqs.(1), (2) and the homogeneous equation for Eq.(3) completely agree with the linear equations formulated to express the flow with alternate bars in straight channels. However, the right hand side of Eq.(3) (the forcing term), which is not equal to 0, gives the deformation effects of channel bending on alternate bars. Eq.(5) below is obtained by eliminating

u_F and v_F from the above three equations and by substituting

$$\eta_F = \eta_{Fb}\sin\left(\frac{\pi}{2}n\right) \tag{4'}$$

derived from the approximation of $n \approx (\pi^2/8)\sin(\pi n/2)$, for η_F.

Although, Parker and Johannesson (10) did not expand these equations with respect to η_F. Then, the authors formulated Eq.(5), referring Kishi'(9) similar expression that was used in an analysis.

$$\eta_{Fb}'' + \frac{r\left\{M_1 + 1 - \frac{P_1}{2P}(M-1) + \frac{\pi^2\Gamma}{8P}\right\}}{\frac{r^2}{2P}(M_1+1)}\eta_{Fb}' + \frac{\frac{\pi^2}{4}\Gamma}{\frac{r^2}{2P}(M_1+1)}\eta_{Fb} = \frac{8}{\pi^2}\frac{D_1 + \frac{r}{2P}D2}{\frac{r^2}{2P}(M_1+1)}\cos\phi + \frac{8}{\pi^2}\frac{D_2 - \frac{r}{2P}D_1}{\frac{r^2}{2P}(M_1+1)}\sin\phi \tag{5}$$

here, $D_1 = r\left\{(M_1+1)(A+F^2) - (M-1)\tilde{b}_C\right\}$; $D_2 = r(M-1)\tilde{a}_C$

Eq.(5) gives the spatial force oscillation. The resonance requirement is that the coefficient of the third term of the left hand side is equal to 1, which gives the wavenumber of the force oscillation. As a result, the resonant wavenumber is determined as follows:

$$r_{res} = \frac{\pi}{2}\sqrt{\frac{2P\Gamma}{M_1+1}} \tag{6}$$

The natural resonant state occurs when the coefficient of the damping term (the second term in the left hand side in Eq.(5)) is equal to zero (equivalent to the neutral condition where the development of the sand bar is halted). Therefore, Parker and Johannesson (10) suggested the following equation as an additional condition for resonance.

$$\Gamma_{res} = \left(\frac{2}{\pi}\right)^2\left\{P_1(M-1) - 2P(M_1+1)\right\} \tag{7}$$

Each value of Γ in the experimental conditions is not always realized to coincide with the value of Γ_{res} calculated from Eq.(7). Thus, the resonant wave number calculated from Eq.(6) by using an ordinary value of Γ is not natural resonant one. However, the resonant wave number obtained from Γ different from Γ_{res} has the content of the resonant wavenumber in a damping oscillation.

Comparison Between the Linear Solutions of Parker and Johannesson and the Experimental Values

The following equation can be obtained by solving Eq.(5) for η_{Fb}:

$$\eta_{Fb} = \frac{\sqrt{E_1^{\,2} + E_2^{\,2}}}{\sqrt{(K_1 \bullet 1)^2 + (K_2 - 1)^2}} \sin(\phi + \phi_1) \tag{8}$$

where,

$$K_1 = \frac{2P(M_1+1) - P_1(M-1) + \frac{1}{4}\pi^2\Gamma}{r(M_1+1)} \; ; \quad K_2 = \frac{\pi^2 P\Gamma}{2r^2(M_1+1)} ; \quad E_1 = \frac{8}{\pi^2}\frac{2PD_1 + rD_2}{r^2(M_1+1)} ;$$

$$E_2 = \frac{8}{\pi^2}\frac{2PD_2 - rD_1}{r^2(M_1+1)} ; \quad \phi_1 = \tan^{-1}\left(-\frac{K_1}{K_2-1}\right) + \phi_0 ; \quad \phi_0 = \tan^{-1}\left(\frac{E_1}{E_2}\right)$$

The curvature-driven bed topography of the bed scoured by the spiral flow is given as follows:

$$\eta_C = -\frac{\pi^2}{8} A \sin\phi \bullet \sin\left(\frac{\pi}{2}n\right) \tag{9}$$

After substituting equation (8) into η_{Fb} of Eq.(4') and then incorporating η_F with Eq.(9), the linear meander bed form $\tilde{\eta}_B$ can be obtained by:

$$\frac{\tilde{\eta}_B}{H} = \psi_0 \sqrt{\left(\frac{\pi^2}{8}A\right)^2 + \frac{E_1^{\,2} + E_2^{\,2}}{K_1^{\,2} + (K_2-1)^2} - \frac{\pi^2}{4} A \sqrt{\frac{E_1^{\,2} + E_2^{\,2}}{K_1^{\,2} + (K_2-1)^2}} \cos\phi_1} \bullet \sin(\phi + \phi_2) \sin\left(\frac{\pi}{2}n\right) \tag{10}$$

where,

$$\phi_2 = \tan^{-1}\left\{ \frac{\sqrt{\frac{E_1^{\,2} + E_2^{\,2}}{K_1^{\,2} + (K_2-1)^2}} \sin\phi_1}{-\frac{\pi^2}{8}A + \sqrt{\frac{E_1^{\,2} + E_2^{\,2}}{K_1^{\,2} + (K_2-1)^2}} \cos\phi_1} \right\} \tag{11}$$

The amplitude A_{11} of the wave (1, 1) of the measured bed topography can be compared with the amplitude of Eq.(10). Because the amplitude varies depending on the coefficient of the damping term, the experimental values are compared in the cases with different values of B/H. Figs. 3 - 6 compare the theoretical values with the experimental ones of r/r_{res} and A_{11}/H which are taken as the horizontal and vertical axes, respectively. At B/H=30, the experimental value of K_1 is close to zero, a natural resonance state theoretically arises and the theoretical value of the amplitude goes to infinity. However, the experimental values of amplitude are distributed with a bell- shape to have the vertex near the resonant wavenumber, where the maximum is about 1. This value is close to

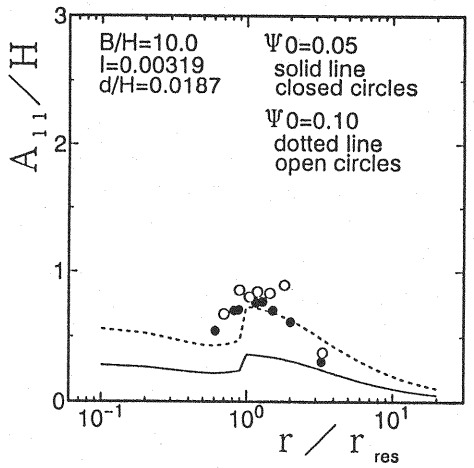

Fig. 3 Comparison of the theoretical amplitude of Parker et al. with the experimental values in the case of B/H = 10

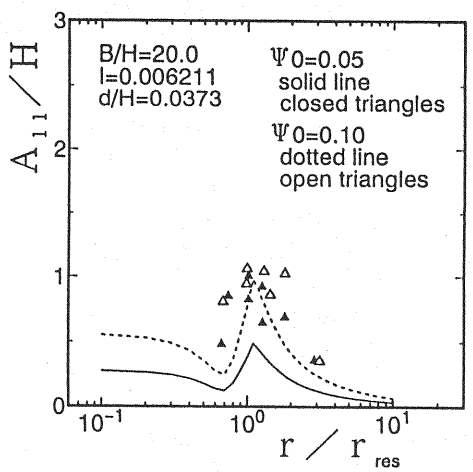

Fig. 4 Comparison of the theoretical amplitude of Parker et al. with the experimental values in the case of B/H = 20

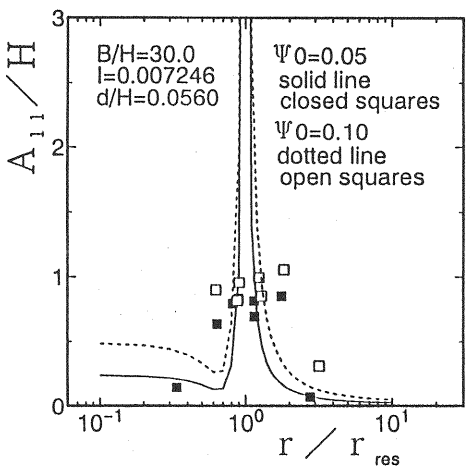

Fig. 5 Comparison of the theoretical amplitude of Parker et al. with the experimental values in the case of B/H = 30

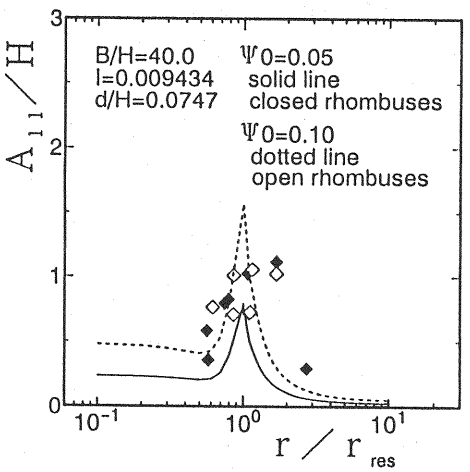

Fig. 6 Comparison of the theoretical amplitude of Parker et al. with the experimental values in the case of B/H = 40

those in other cases. Conversely, at $B/H = 40$, where the formation of alternate bars is theoretically possible ($K_1(0)$), the theoretical values approximated by a finite curve has the maximum at the resonant wavenumber. Also, distribution of the measured values is similar to that of the theoretical values. Interesting cases are $B/H = 10$ and 20, where $K_1 > 0$ and theoretically alternate bars cannot form. In both cases, theoretical results take a maximum near the resonant wavenumber, and the measured values are located around the theoretical values. This demonstrates that the meandering wavelength, which causes the dangerous bed scouring, can exist even under conditions where alternate bars are not formed. Even so, the meandering wavelength has been believed to arise only when the formation of the sand bar and bed scouring due to bending occur simultaneously.

However, the acceleration term and the transverse gradient term of the water surface in the flow motion equations were neglected in the theory of Parker and Johannesson (10) to address the resonance phenomenon straightforward. As a result of this gross oversimplification, the factors related to alternate bars, such as the absence of the dominant wavelength of alternate bars, can be roughly discussed. At $B/H=20$, the formation of weak alternating bars was evident in the experiment. The experimental values in this case are considered to indicate the coexistence of alternate bars and meandering. To answer these questions, the experimental values are compared with the theoretical solutions by Hasegawa (5) in the next section.

Comparison of the Theoretical Values of Hasegawa with the Experimental Values

Parker and Johannesson (10) neglected $\partial v/\partial s$ and $\partial \xi/\partial n$ (transverse water surface gradient) in the equations, but Hasegawa (5) retained them in the expansion of the equations. Additionally, the alternate bars had a dominant wavenumber. Differing from Parker and Johannesson, Hasegawa used an approximation method of Galerkin and the different ways of expressing the secondary flow. Since η is directly calculated from one of his equations, a clear understanding of η_F and η_C is difficult, unlike the force oscillation equation. Due to space limitation, only the results can be mentioned and the equation for the (1, 1) wave is shown as:

$$\frac{\tilde{\eta}_B}{H}=\sqrt{\frac{K^2+\Lambda^2}{\kappa^2+\lambda^{*2}}}\cos\{k(s-\sigma)\}\sin\left(\frac{\pi}{2}n\right) \tag{12}$$

here, $\kappa = M\left(b_{11}-\frac{5}{3}\sqrt{C_{f0}}\right)+\frac{\pi}{2\gamma k}c_{11}$; $\lambda^*=Ma_{11}-\frac{\pi}{2\gamma k}d_{11}-\frac{\pi^2}{4\gamma^2 k}\sqrt{\frac{\tau^*_c}{\mu_s\mu_k\tau^*_0}}$;

$K=\frac{\psi_0}{\gamma}\left(Mb'_{11}+\frac{\pi}{2\gamma k}c'_{11}\right)$; $\Lambda=\frac{\psi_0}{\gamma}\left(Ma'_{11}-\frac{\pi}{2\gamma k}d'_{11}+\frac{\pi}{2\gamma k}N_{11}\right)$; $k=\frac{2\pi H}{\tilde{\lambda}}$; s = longitudinal coordinate normalized by H ; N_{11}= the coefficient of the strength of the secondary flow, to which a value of 14 was assigned; $a_{11}, a'_{11}, b_{11}, b'_{11}, c_{11}, c'_{11}, d_{11}$ and d'_{11} are complicated equations with respect to k, M, γ, F and C_{f0}, those correspond to the coefficients of the solutions for u_F and v_F; σ= the phase lag taken in s-axis. The other notations are the same as the previous ones.

The conditions corresponding to the state of resonance for Eq.(6) can be obtained from $\lambda^*=0$. This will be accepted from the comparison of equation (8) with Eq.(12). It is difficult to find k analytically to fulfill these conditions, because a_{11} involves higher order terms for k. Therefore, k was directly assigned to the horizontal coordinate to compare the amplitude of Eq.(12) with the experimental values (Figs. 7-10). The figures show that resonance occurs at B/H = 20.0, which differs from the previous case, because the neutral line for the formation of alternate bars shifted due to the rescaling of the model. Additionally, because a weak sand bar formation was observed in the experiment, the solutions of Hasegawa (5) are closer to the actual phenomenon. Thus, the natural resonance state arises at B/H= 20.0 according to the linear theory. The experimental values produce an upward convex curve, but the maximum value is only as large as 1.0, which is not particularly different from other cases. At B/H= 10, the non-formation of alternate bars, the solutions of Hasegawa (5) also produce an upward convex curve, which supports the validity of the

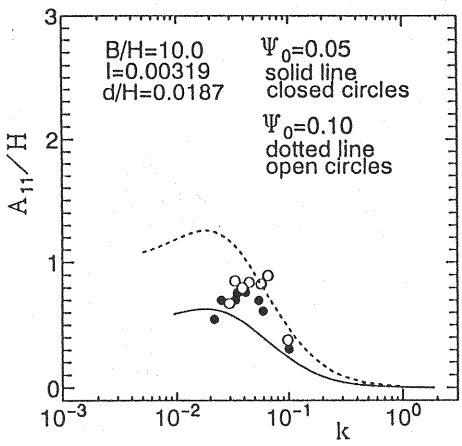

Fig. 7 Comparison of the theoretical amplitude of Hasegawa with the experimental values in the case of B/H = 10

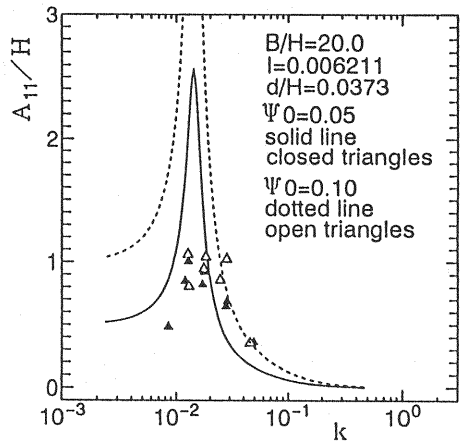

Fig. 8 Comparison of the theoretical amplitude of Hasegawa with the experimental values in the case of B/H = 20

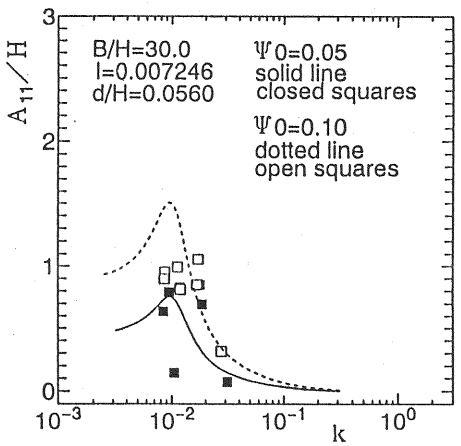

Fig. 9 Comparison of the theoretical amplitude of Hasegawa with the experimental values in the case of B/H = 30

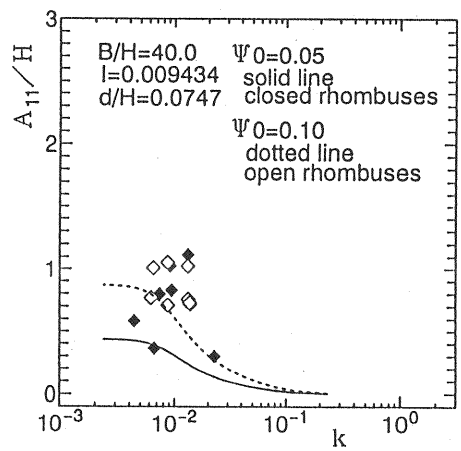

Fig. 10 Comparison of the theoretical amplitude of Hasegawa with the experimental values in the case of B/H = 40

experimental values. However, the maximum point of Hasegawa (5) deviated slightly from the experimental one. This tendency can also be seen at $B/H = 30$ and 40, where alternate bars are formed in the Hasegawa theory. The greater the parameter affecting the growth rate of the alternate bars (λ^*) is, the smaller the theoretical maximum value becomes, which is comparable to the solutions of Parker and Johannesson. This may appear illogical and is discussed later in this paper.

PHASE LAGS IN THE LINEAR SOLUTIONS AND THE EXPERIMENTS

The phase lag of the (1, 1) wave in the solutions of Parker and Johannesson (10) is given by ϕ_2 of Eq.(11), which was compared with the experimental values. In the experiment, an apex of the meandering bend was assumed to be the origin. The distance between the origin (apex) and the bed scouring downstream was measured as positive and upstream was measured negative in the horizontal direction. In addition, the bed scouring was positive in the vertical, downward direction.

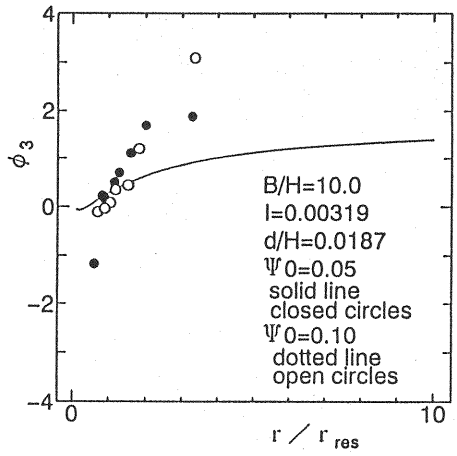

Fig. 11 Phase lag of A_{11} wave from the apex of meandering channel in the case of B/H = 10

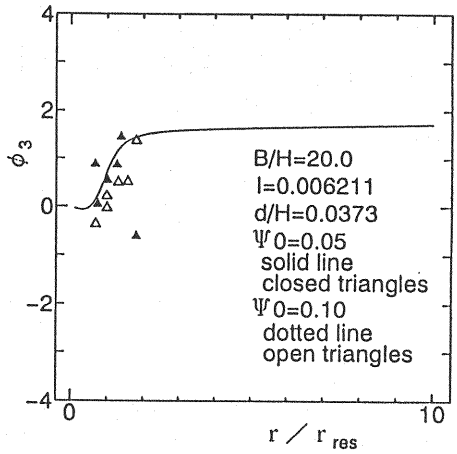

Fig. 12 Phase lag of A_{11} wave from the apex of meandering channel in the case of B/H = 20

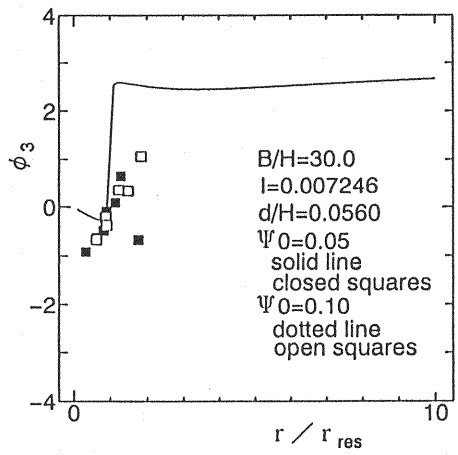

Fig. 13 Phase lag of A_{11} wave from the apex of meandering channel in the case of B/H = 30

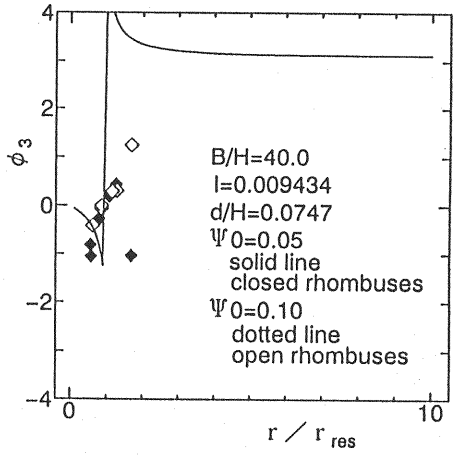

Fig. 14 Phase lag of A_{11} wave from the apex of meandering channel in the case of B/H = 40

The theoretical values were also adjusted accordingly. The theoretical phase lag ϕ_2 was converted to ϕ_3, which is equal to $(\pi - \phi_2)$, to compare them with the experimental values.

The results are shown in Figs. 11-14. Except when $B/H = 10$, where alternate bars do not form, the results are almost consistent. The experimental values show that with non-formation of alternate bars, considerable bed scouring occurs downstream, sometimes reaching the point of inflection and even to the vertex of the convex bank. The theoretical convex curves, however, do not go beyond the inflection point (approximately $\pi/2$).

Both the theoretical and experimental values show that at $B/H = 20$, 30 and 40 with formation of alternate bars, bed scouring takes place only near the apex of the concave bank. It is interesting that on the bed topography where alternate bars formed, bed scouring occurred upstream from the apex in the meandering channel whose wavelength was longer than the resonant wavelength, which is also supported by the experimental values.

DISCUSSIONS

In damping term of Eq.(5), factor K_1 is a parameter of the growth rate of alternate bars. Therefore, at $K_1 = 0$, where the natural resonance state appears, the bed topography is neutral and is stable against disturbance. This can be interpreted that when external forces are exerted, the bed topography is deformed by the force without any resistance.

When K_1 is positive, the bed topography is stable against disturbance and negative acceleration acts against the deformation caused by external forces. However, the response amplitude has a maximum value at a certain wavenumber. Thus, the resonant nature inherently exists in alluvial meandering channels. And also, in this case, the homogeneous solutions of Eq.(5) (free oscillation) corresponding to the self-excited wave of the river bed damp together with the distance from the origin, because the homogeneous solution has the form $\eta_{Fb} = \exp\left\{1/2\left(-K_1 \pm \sqrt{K_1^2 - 4K_2}\right)\phi\right\}$. Therefore, only the particular solution of Eq.(8) should be considered.

When K_1 is negative, the river bed is unstable and alternate bars begin developing. In this case, the homogeneous solutions increase together with the distance from the origin. As a result, the self-excited wave of the bed disproves the solution of Eq.(8), and they lose their significance, which technically indicates that the linear theory cannot strictly be applied in this case. The experimental values in the regions where alternate bars form are apparently consistent with the solution of Eq. (8), probably because the formation of the alternate bars is halted by other factors (nonlinear factors) and creates a situation equivalent to the homogeneous solutions not being used. The high applicability of the phase solution implies that this interpretation is somewhat legitimate. In other words, an inherent peculiar system acts to cease the growth of alternate bars at a limited amplitude, which might deter deformations of alternate bars caused by external forces, as if it was a damping effect.

SUMMARY

A total of 80 experiments were conducted in meandering river channels, combining different maximum dimensionless bend curvatures, dimensionless meandering wavenumbers, and the width-depth ratios. The equilibrium bed topography data obtained in the experiments were analyzed by linear theories. As a results, the following conclusions were reached:

(1) In the major waves to comprise the bed form, the amplitudes of (2, 0) and (3, 1) waves were not particularly affected by the bend. However, they varied with the parameters relevant to the growth rate of alternate bars, such as the width-depth ratio. The amplitudes of the (1, 1) and (2, 2) waves changed primarily with the dimensionless meandering wavenumber and had a maximum value at a certain wavenumber. In the context of the linear theory, the resonant state should be discussed only on the sand bar which is influenced by the curvature of the (1, 1) wave (excluding the portion of bed scour with the direct influence of the curvature).

(2) The linear solutions of Parker and Johannesson (10) and Hasegawa (5) show the natural resonance wavenumbers under neutral conditions where the growth rate of alternate bars is zero. However, the experimental values of the amplitude under these conditions do not largely exceed unity in normalized scale with mean water depth. They are differ little from the values of the amplitude under other conditions.

(3) The convex curves representing the amplitude tended to show peaks near the resonant wavenumbers, even under the conditions where alternate bars do not grow. This is regarded as an inherent nature of alluvial meandering river beds.

(4) The linear solutions were essentially invalid for condition with the formation of alternate bar, but

the experimental values agree well with the particular solution. This may be due to non-linear factors influencing the prevention of sand bar growing.
(5) The phase solutions of the linear equation corresponded very well with the measured phase of the (1, 1) wave. The agreement was better in areas where linear solutions were problematic where alternate bars grow. Conversely, it was worse in areas where linear solutions were not problematic where alternate bars did not grow.

Since this paper discusses linear theory, the (1, 1) wave inevitably is the only wave subject to discussion. Nonlinear analyses are absolutely necessary for a discussion of the other component waves. For such a discussion, the formation of alternate bars and the nonlinear effects of meandering should be dealt with separately. This will be subject of future research for the authors.

REFERENCES

1. Blondeaux, P. and G. Seminara: A unified bar-bend theory of river meanders, Journal of Fluid Mechanics, Vol.112, pp.363-377, 1985.
2. Colombini, M., G. Seminara and M. Tubino: Finite-amplitude alternate bars, Journal of Fluid Mechanics, Vol.181, pp.213-232, 1987.
3. Engelund, F.: Flow and topography in channel bends, Journal of the Hydraulics Division, ASCE, Vol.100, HY11, pp.1631-1648, 1974.
4. Garcia, M. and Y. Nino: Dynamics of sediment bars in straight and meandering Channels: Experiments on the resonance phenomenon, Journal of Hydraulic Research, IAHR, Vol.31, pp. 739-761, 1993.
5. Hasegawa, K.: A study on flows and bed topographies in meandering channels, Proceedings of JSCE, No.338, pp.105-114, 1983 (in Japanese).
6. Hasegawa, K. and K. Nakamura: Interacting process of free and forced bars in systematic meandering experiments with resonant bed scours, Proceedings of Hokkaido Branch of JSCE, No.49, pp.433-438, 1993 (in Japanese).
7. Hasegawa, K. and K. Nakamura: Harmonic analysis on free and forced bar forms in experimental meandering channels with resonance condition, Proceedings of Hokkaido Branch of JSCE, No.50, pp.498-503, 1994 (in Japanese).
8. Kinoshita, R.: Research on the transition of the channel of the Ishikari River, Material No.36, Office of Resources of the Science and Technology Agency, 1961 (in Japanese).
9. Kishi, T.: Progress of research on flow and bed topography in a bed of rivers, Proceedings of the Fourth Conference on Rivers and Dams (Sapporo), The River Bureau of the Ministry of Construction, pp.23-45, 1988 (in Japanese and Chinese).
10. Parker, G. and H. Johannesson: Observation on several recent theories of resonance and overdeepening in meandering channels, River Meandering Water Resources Monograph 12, AGU. Chpt.12, pp.379-415, 1989.
11. Seminara, G. and M. Tubino: Rizonanza non lineare in meandri di ampiezza finita. parte prima: Theoria, Atti XXII Convegno di Idraulica e Construzioni Idrauliche, Cosenza, 1990.
12. Struiksma, N., K. W. Olesen, C. Flokstra and H. J. De Vriend: Bed deformation in curved alluvial channels, J. Hydraulic Res., 23(1), pp.57-59, 1985.
13. Toyabe, T., Y. Watanabe, Y. Shimizu, K. Hasegawa and K. Nakamura: Hydraulic model experiments with a movable bed in a meandering water channel, Proceedings of Hokkaido Branch of JSCE, No.49, pp.445-450, 1993 (in Japanese).
14. Toyabe, T., Watanabe, Y., Shimizu, K. Hasegawa and K. Nakamura: Hydraulic model experiments with a movable bed in a meandering water channel (No. 2), Proceedings of Hokkaido Branch of JSCE, No.50, pp.520-525, 1994 (in Japanese)

APPENDIX --- NOTATION

The following symbols are used in this paper:

$\tilde{a}_C$, $\tilde{b}_C$	= parameters of the secondary approximate solution of Engelund related to u_C;
A_s	= dimensionless coefficient concerned with correlation between the main flow and secondary flow;
A	= dimensionless bed scour factor;
A_{ij}	= amplitude of (i,j) component in bed topographical waves;
$(A_{ij})_T$	= A_{ij} of the alternating bar in a straight channel;
$(A_{ij})_F$	= A_{ij} of the alternating bar affected by a channel bend;
$(A_{ij})_C$	= A_{ij} of the bed form scoured by the secondary flow in a channel bend;
b	= half-width of a channel;
B	= width of a channel;
C_{f0}	= frictional coefficient for the mean flow;
D_1, D_2	= dimensionless parameters in (5);
E_1, E_2	= dimensionless parameters in (8) ;
F	= Froude number of the base flow;
$\tilde{h}_C$, h_C	= perturbation of water depth affected by the channel bend, the dimensionless form made with $\Psi_0 H$;
H	= depth of the base flow;
k	= dimensionless wavenumber of a meandering channel $2\pi H/\tilde{\lambda}$;
K_1, K_2	= dimensionless parameters in (8);
M, M_1	= dimensionless coefficients in the equation of sediment continuity;
$\tilde{n}$, n	= transverse coordinate, and the dimensionless form with the channel half-width $\tilde{n}/b$;
N_{11}	= coefficient with respect to the secondary flow intensity near the bed;
P, P_1	= dimensionless coefficients in the equation of downstream momentum balance;
r	= dimensionless wavenumber of a meandering channel $2\pi H/(\tilde{\lambda} C_{f0})$;
r_{res}	= dimensionless resonant wavenumber;
r_{Cmin}	= minimum centerline radius of curvature;
$\tilde{s}$, s	= longitudinal coordinate along the centerline of a channel, and the dimensionless form with the base flow depth $\tilde{s}/H$;
u_C, u_F	= scaled dimensionless longitudinal velocity perturbations in the "C" and "F" problems, respectively;
$\tilde{u}_C$, $\tilde{u}_F$	= longitudinal velocity perturbations in the "C" and "F" problem, respectively;
U	= cross-sectional mean velocity of the base flow;
v_C, v_F	= scaled dimensionless transverse velocity perturbations in the "C" and "F" problems, respectively;
$\tilde{v}_C$, $\tilde{v}_F$	= transverse velocity perturbations in the "C" and "F" problem, respectively;
β	= coefficient in transverse sediment transport;
γ	= ratio of half-width to base flow depth b/H;
Γ , Γ_{res}	= coefficient of gravitational diffusion $\beta/(\gamma^2 C_{f0})$, and value of Γ in resonant state;
$\tilde{\eta}_B$	= displacement of bed topographical surface from the mean bed elevation in a meandering channel with alternating bars;
η_C	= scaled displacement with $\Psi_0 H$ of bed topographical surface from the mean bed elevation in "C" problem;
$\tilde{\eta}_F$, η_F	= displacement of bed topographical surface from the mean bed elevation in "F" problem, and the scaled form with $\Psi_0 H$;
η_{Fb}	= amplitude function with respect to ϕ in η_F;
κ , K	= dimensionless parameter in (12) of Hasegawa theory;
λ^* , Λ	= dimensionless parameter in (12) of Hasegawa theory;
$\tilde{\lambda}$	= meandering wavelength;
μ	= dynamic Coulomb frictional coefficient;
σ	= phase lag taken in s-axis;
τ^*_c	= dimensionless critical shear stress;

τ^*_{s0} = dimensionless shear stress for the base flow;
ϕ = dimensionless longitudinal phase coordinate $2\pi\tilde{s}/\tilde{\lambda}$;
ϕ_0 = phase lag given by $tan^{-1}\{E_1/E_2\}$;
ϕ_1 = phase lag given by $tan^{-1}\{-K_1/(K_2-1)\}$;
ϕ_2 = phase lag given by (11);
ϕ_3 = $\pi - \phi_2$;
Ψ_0 = dimensionless maximum centerline curvature b/r_{Cmin};

(Received January 5, 1996; revised January 12, 1998)